SEISMIC ANALYSIS OF THE SYLMAR INTERSTATE 5 AND HIGHWAY 14 CONNECTOR BRIDGE

Robert K. Dowell

Dowell-Holombo Engineering, Inc.
Department of Structural Engineering
University of California, San Diego

Abstract

This paper presents measured and analysis time-history results of the heavily instrumented 10-span North Connector Bridge (53-2795F) at the 5/14 Interchange, subjected to the M7.1 Hector Mine earthquake. Relatively simple spine and more detailed shell element models were developed. Measured base motions were used as input for the finite element models, with absolute and relative superstructure displacement time-histories compared to measured responses. Results show that 5% equivalent viscous damping is realistic, as is the concrete strength of 5 ksi. It was found that the rotational mass inertia of the superstructure is an important quantity for spine models of single-column-bent bridges.

Introduction

The California Strong Motion Instrumentation Program (CSMIP) has been measuring the behavior of bridges subjected to earthquakes for several years, allowing researchers and practitioners to better understand the (1) seismic behavior of various types of bridge structures and (2) capabilities of their analysis tools to properly model the seismic response of bridges. The end result is improved seismic bridge design and analysis, with increased safety against structural failure and associated loss of life, as well as significant savings to the State from more efficient designs. The State of California has instrumented over 60 bridges, providing measured accelerations at various locations on the structure and in its vicinity. Displacement and velocity time-histories are determined from integrating and filtering measured accelerations. Herein the term “measured” is applied to recorded accelerations as well as to velocities and displacements that were derived from these accelerations. Strictly speaking, however, only the accelerations were measured. In this project, the focus is on the seismic response of a single prestressed concrete, box-girder connector bridge, discussed in the following.

The 1582 ft long, 10-span, 5/14 North Connector Bridge (Bridge No. 53-2795F) has been heavily instrumented with 42 sensors that measure seismic accelerations at various locations on and below the bridge, including the (1) superstructure, (2) abutments and (3) columns. Sensors were also placed 91 ft below ground in the large-diameter CIDH shaft of Bent 7 and at a free-field location adjacent to Abutment 1. In the time since the bridge was constructed and instrumented in 1994, several small earthquakes produced large enough accelerations to automatically turn on, or trigger, the instrumentation and begin recording data. Once triggered, all of the instrumentation is activated and recorded for the duration of the earthquake.

For the North Connector Bridge, three earthquakes are listed in the CSMIP database. Of these records, only the Magnitude 7.1 Hector Mine Earthquake was considered as it resulted in 50 times larger structure displacements than the other two earthquakes. This earthquake occurred on October 16, 1999 with the epicenter 47 miles ESE of Barstow. Various photographs showing different views of the connector bridge and 5/14 Interchange are given in Figures 1 through 4.

The purpose of this study is to use the measured strong motion data of the 2-frame, 10-span connector bridge to determine how well the seismic behavior of a long connector bridge can be captured by a global bridge analysis model and to determine what level of sophistication is required in the analysis (spine model versus shell model). Several studies have focused on the 2-span Painter Street Bridge [1], but this is the first study to compare measured and analysis results of a much longer, single-column-bent connector bridge. Initially, the complete structure was modeled with beam elements and compared to measured results. A more detailed structural model was then developed that consisted of shell elements for the superstructure and bent caps with beam elements for the columns and large-diameter shafts.

Measured data and analysis model results demonstrate that the two bridge frames are uncoupled from each other due to the unique expansion joint between frames (Figure 4). This allowed the shell model to be developed for only one frame, without any loss in accuracy, in order to compare its behavior to both measured and spine model results. As Frame 1 spine model results compared well to measured behavior, and more sporadic comparisons were found for Frame 2 due to soft soil at three of the bents in this frame, it was decided that little would be gained by modeling Frame 2 with shell elements. Therefore, a more detailed shell model was developed for Frame 1 only, with no loss of accuracy by not including both frames in the model.

Typically, an expansion joint is placed at the approximate dead load point-of-inflection in a span (about 20% of the total span length), with the result that the long span sits on a hinge seat provided by the short span. Since the previous bridge at this site failed by unseating of the long span at the hinge, the new hinge detail has two closely spaced columns at Bents 5 and 6, with short cantilever spans that do not touch at the middle, resulting in a several inch gap between frames and no shear transfer between them (Figure 4). Thus it is not possible for this bridge to have failure from unseating of a span at the hinge, since neither span is supporting the other. As the bridge displacements were relatively small from the Hector Mine Earthquake, the frames never came into contact. Measured time-history results on both sides of the hinge clearly show this, with adjacent frames moving independently of each other at different natural periods. It is important to note, however, that while the frames did not contact each other in the Hector Mine Earthquake, they will bang into each other when subjected to larger and/or closer earthquakes in the future.

Instrumentation

Instrumentation locations for the bridge are given in Figure 5. For the North Connector Bridge, 42 channels of acceleration data were recorded from the Hector Mine Earthquake. This provided valuable measured data of transverse bridge response at each bent, as well as longitudinal and transverse responses at both abutments and the base of some of the columns.

Vertical behavior was recorded at several locations. Measured displacements at the abutments and the base of Bent 5 were used to develop unique input motions for all of the supports in the analysis models.

Computational Models

Spine Model

For seismic bridge design the basic analysis tool is a spine model that represents the bridge superstructure, columns and shafts with beam elements positioned along the centroid of each member (Figure 6). For the North Connector Bridge, a series of beam elements were used to model the prestressed concrete, multi-cell box girder superstructure. Due to the 3-D nature of the curved bridge and applied loading, 3-D beams were required which have 3 translational and 3 rotational displacement degrees-of-freedom at each end, for a total of 12 degrees-of-freedom for each beam element. General beam sections are defined by their area and inertia in both principal directions as well as the torsional constant. For the spine model these section properties were calculated by hand as the SAP computer program [2] could not generate them automatically, as it can for many other shapes. In addition, the section description requires that the concrete material property be given, allowing distributed mass and weight to be automatically included. The general-purpose finite element program SAP2000, Version 8 [2] was used for all analyses presented in this paper.

From comparing time-history analyses and measured results it was determined that the unconfined concrete strength was 5 ksi at the time of the measured earthquake. This is a reasonable increase to the 28-day concrete strength of 4 ksi listed on the bridge plans for the superstructure, columns and shafts, and matches the Caltrans recommended value for seismic analysis and design [3]. As discussed later, however, only after fully developing the shell model, and comparing these results to spine model and measured results, was it realized that the modulus of elasticity must be larger than the ACI value [4] for an unconfined concrete strength of 5 ksi.

The ACI modulus of elasticity [4] is based on a secant stiffness through 50% of the concrete strength. However, for this analysis the initial modulus of elasticity is required rather than the standard ACI value due to the nonlinear stress-strain curves of concrete and the low concrete stresses from the earthquake. The initial modulus is reported in [5] to be about 10% higher than the ACI value [4]. Thus the modulus of elasticity used in all reported analyses is 10% higher than the ACI value based on a 5 ksi concrete. Concrete weight is taken as 150 pcf and unit mass is this weight divided by gravity of 32.2 ft/s^2.

Initially, modal and time-history results did not match between the spine and shell models. To better understand these initial, and unexpected, differences, separate breakout spine and shell models were developed of a single, straight, box-girder span. This allowed modes shapes, mass distribution and stiffness characteristics to be compared more directly. It was found that mass and stiffness values of the breakout models agreed well, but that there were large differences in the modal behavior; no torsional mode developed for the breakout beam model, whereas this was the primary response of the breakout shell model. This is interesting because

the shell model has only translational mass terms, with no rotational mass included. However, since the mass is distributed across the width and height of the shell model superstructure, rotational mass inertia naturally develops about the centroidal axis of the member, based only on translational mass terms. To verify this, the rotational mass of the box-section was calculated by hand about its centroidal axis and then lumped at each node of the breakout spine model. Results from this analysis showed that the breakout spine model now had the same torsional mode and period of vibration as the breakout shell model.

To more directly compare the behavior of the spine and shell models, a second spine model was developed by eliminating Frame 2 from the original complete spine model (the shell model was developed only for Frame 1). Spine and shell models are shown in Figures 7 and 8. Rotational mass inertia values were computed by hand for each superstructure node and added to the Frame 1 spine model, resulting in similar mode shapes and natural periods as the shell model (see Figure 9 for direct comparisons of Modes 1 through 3). These results demonstrate that the bridge mass, stiffness and boundary conditions have been realistically modeled.

Including rotational mass increases the 1st Mode transverse period of the spine model by 3.4%. Without rotational mass included, the Frame 1 spine model still develops a transverse 1st Mode response. This is because the 1st Mode is a combination of transverse column bending and torsion of the superstructure. Thus the translational mass is also important in this mode. As discussed previously with regard to the breakout spine model, a straight bridge that is constrained to allow a pure torsion mode will not develop this mode and will have no torsion response if rotational mass is not provided. For the Frame 1 spine model this makes some difference, but not nearly as dramatic a difference as with the breakout spine model.

Following initial time-history analyses of Frame 1 it became clear that there were two quantities that still needed to be defined for the connector bridge: The level of equivalent viscous damping and the modulus of elasticity of concrete. Frame 1 was used for these assessments because the shafts are founded in rock and do not have the added unknown soft soil properties at Bents 7, 8 and 9 of Frame 2. Any conclusions about damping and concrete properties found for Frame 1 should be equally valid for Frame 2 and, therefore, are applied to both frames. The multi-support ground input is defined by measured displacements at the abutments and base of Bent 5. Each bent is provided with unique time-history base motions in the global longitudinal and transverse directions. Base motions are applied to the ends of soil springs that are connected to the large-diameter shafts. Damping primarily affects the magnitude of response while the modulus of elasticity primarily affects the natural period.

Absolute measured transverse deck displacements at Bent 5 are compared to analysis results with 4, 5 and 6 ksi concrete strengths (E is increased over the ACI value by 10% for all cases, as discussed elsewhere) and 5% damping in Figure 10. Based on the closest period response, these results suggest that the bridge had a 5 ksi concrete at the time of the earthquake. The most realistic equivalent viscous damping value was determined in a two-part process. Initially, 2%, 5% and 10% damping (constant for all modes) was considered (Figure 11). These results indicate that the best value of damping is somewhere between 2% and 5%, with 10% damping resulting in reduced magnitudes and damped-out vibrations, and 2% causing more oscillations and larger magnitude response than measured. A second set of analyses was

conducted to refine the damping levels further, allowing time-history comparisons at 3%, 4% and 5% damping, with 5% providing slightly better results.

This 5% damping value is consistent with Caltrans recommendations and seismic design practice, and appears to be the best overall value based on the time-history comparisons discussed above. Note that both modal and direct-integration time-history analyses were conducted and it was found that the results were very close to each other, with modal analyses producing a much quicker solution. An added advantage of modal time-history analysis is that it is possible to specify constant damping for all modes, whereas for direct integration a mass and stiffness proportional damping is used. Coefficients for Rayleigh damping were found by setting the damping to 5% at periods of 0.5 and 1.5 seconds. Between these periods the damping reduces to a low of about 4%. However, time-history results were virtually identical between direct integration with Rayleigh damping and modal analysis with 5% damping for all modes. Thus, modal analysis with constant 5% damping was used for all time-history results presented herein. The minimum number of modes specified for the complete spine model and the Frame 1 spine model was 50 and 20, respectively. Close comparisons to direct integration demonstrated that more modes were not required.

Absolute and relative transverse deck displacement time-histories at Bent 5 are compared between the (1) spine model with rotational mass, (2) spine model without rotational mass and (3) more detailed shell model (Figures 12). These results clearly show the importance of including superstructure and bent cap rotational mass in a spine model for seismic analysis of a typical connector bridge that has single-column-bents, resulting in very similar behavior between the spine model and more detailed shell model. With rotational mass not included the spine model transverse displacements are often smaller than measured and shell model results. Adding rotational mass will be even more important for intermediate frames of long, multi-frame, single-column-bent viaducts that do not have the beneficial restraint from abutments. However, this may not be so important for multiple-column-bent structures since the superstructure will tend to stay flat as it moves transversely.

Columns were modeled with beam elements, as were the large-diameter pile shafts. In design, the column lengths were extended at Bents 2, 3, 4 and 10 by providing isolation casings over the top 30 ft of soil to allow these regions to move freely, resulting in similar stiffness to the columns along each frame of the structure. This results in improved seismic response with no single bent or column being overloaded. All of the bent shafts for Frame 1 are embedded in hard rock-like soil, based on the log-of-test-borings shown on the plans. The soil springs are very stiff at these rock sites compared to sand. By running several analyses with the full range of possible soil spring stiffness values, it was determined that these variations have little effect on the response of the structure, in terms of natural periods and time-history displacement traces. Spring constants were based on recommended values provided in the LPile User's manual [6].

In order to capture the proper natural mode shapes and periods and to have a reasonable distribution of mass, the superstructure spans were modeled with 4 beams, columns with 3 beams and large-diameter shafts were modeled with multiple elements at 10 ft spacing between nodes to allow for interaction with longitudinal and transverse soil springs. Ground motions were applied

to the spring ends at all bents and to the abutments. Lateral spring stiffness' were provided in mutually perpendicular directions at 10 ft spacing

Note that the spring constant represents the initial stiffness given in [6], with nonlinear soil behavior not included in the model as the motions were relatively small: Initial elastic stiffness values provide a good representation of the soil behavior throughout the loading. As presented above, three of the Frame 2 column shafts were founded on soft soil above the rock-like material. Based on the log-of-test borings and Frame 2 analysis results from the spine model, the soft soil was taken to be loose sand (defined in [6]). Below the water table the spring stiffness values were reduced, as suggested in [6]. Spine model behavior was compared to measured time-history results of Frame 2 for various soft soil properties at Bents 7, 8 and 9. It was found that the loose sand assumption provided the best overall spine model results for Frame 2, but still not as good as the excellent analysis results for Frame 1. For the spine model, the added weight and mass of the bent caps and soffit flares were lumped at the top of the columns, including the rotational mass of the bent cap about the axis of the superstructure.

Shell Model

The shell model is similar to the Frame 1 spine model discussed above, with the exception that the beam elements representing the bridge superstructure have been replaced by shell elements (compare Figures 7 and 8). Shell elements combine plate and membrane behavior into one element. Rather than determining the section properties by hand, such as area, inertias and torsional constant, and then assigning these properties to the beam elements, the shell elements are positioned to completely define the section geometry, including the deck, soffit, girders and overhangs. So long as the elements are given the correct thickness and location in 3-D space they automatically develop the correct behavior of the structure (this is why the shell model is a good verification for the spine model). Shell elements were also used to model the bent caps and end diaphragms. The columns and large-diameter pile shafts are modeled identically to the spine model. To reduce local shell deformations at the base of the cap/column joint, the column was extended to the top of the superstructure and connected to top and bottom nodes of the bent cap. Within the bent cap, a material property that has no mass and weight was assigned to the column elements so that the concrete would not be included twice in these joint regions.

Since the Frame 1 spine model results matched measured results better than the more variable Frame 2 spine model results, it was decided to develop the shell model only for Fame 1. This produced Frame 1 shell model results that are identical to having both frames included in the shell model, since there is no interaction between frames from the Hector Mine Earthquake.

Boundary conditions of the shell model are similar to the spine model. At the abutment the width and depth of the shell model presented some difficulty in providing the same restraints and releases: The shell model is constrained directly under the girder lines at the soffit level in the longitudinal, transverse and vertical directions. By not constraining the deck or girders, the superstructure is free to rotate in the principal direction but constrained in the other directions, as is the spine model. Along the large-diameter shafts the boundary conditions and applied time-

history ground motions are identical between the two models. Material properties and damping are the same as previously discussed for the spine model.

Time-History Analysis Results

This section compares measured absolute and relative (between deck and ground) time-history results from the (1) spine model and (2) more detailed shell model. Relative displacements between the superstructure and ground are important as they define the deformations and damage of the bridge columns. Absolute and relative time-history displacements for all columns are given elsewhere [7].

Frame 1 spine model analyses were used to define the damping level, modulus of elasticity and concrete strength for (1) Frames 1 and 2 of the spine model and (2) the more detailed shell model that was developed for Frame 1 only. This is because several large-diameter shafts of Frame 2 were placed in soft soil, rather than the rock-like material found at all other locations. Uncertainty from soft and unknown soil properties resulted in sporadic comparisons to measured time-history results associated with arbitrary modifications to the soil properties. This provided little confidence that the damping level and concrete strength could be defined with reasonable accuracy from these Frame 2 time-history analyses. Thus the Frame 1 analyses served to define the damping and concrete properties for both frames and both types of models, removing some of the uncertainty in the analysis of Frame 2.

Results from the spine and shell models indicate that the transverse deck response at Bent 4 (absolute and relative) closely resembles the measured response in magnitude and form for the 25 seconds of recorded strong earthquake motion (Figures 13 and 14), clearly showing that the chosen level of damping and concrete modulus of elasticity are reasonable. Note that dead load sidesway displacements were removed from all analysis results presented herein, unless otherwise indicated, as they were not in the recorded data. This is because any developed sidesway occurred at the time of construction, following the removal of falsework that supported the structure.

Overall comparisons between measured and shell model Frame 1 relative transverse bridge responses are given from 25 to 50 seconds of strong earthquake shaking in Figure 15. Such plots allow all of the measured transverse bent results (bottom figure) to be compared to analysis results (top figure) on a single page. The similarity between measured and analysis plots is quite remarkable, demonstrating that relatively simple analysis models are very capable of realistically capturing the complete response of a bridge structure of this type. Note that the overall transverse response of Frame 1 from the spine model was very similar to the shell model results presented in Figure 15.

The overall period of vibration, form and magnitude of response is very good for the full 25 seconds of strong earthquake loading. These excellent results give further validation of the damping level and concrete properties derived from the Frame 1 spine model analyses and used in the shell model discussed here.

Developing the shell model for Frame 1 proved to be an excellent exercise, demonstrating the capabilities of both shell and spine models to capture measured dynamic time-history responses of a multi-span, prestressed concrete, box-girder connector bridge. It also resulted in the discovery of a significant shortcoming of typical spine modeling procedures for single-column-bent bridges, relating to the inherent lack of rotational mass of the superstructure and bent caps. Results demonstrated that this difficulty is resolved by adding rotational mass of the superstructure to the nodes of the spine model, with excellent comparisons to shell model and measured behaviors.

Measured results indicate that, overall, the shell model is slightly better at capturing the response of the bridge, especially in the axially stiff longitudinal direction. Transversely, there is very little difference between shell and spine model results, so long as rotational mass is included in the spine model.

Conclusions and Recommendations

Acceleration time-history measurements taken on and around the North Connector Bridge of the 5/14 Interchange, from the 1999 Hector Mine Earthquake, have provided immensely valuable information for verifying seismic analysis and design tools that are required for California bridge projects. This structure, in particular, is of interest because it is a heavily instrumented, 10-span, 2-frame connector bridge, with single-column-bents and variable ground motion, requiring multiple support excitations to be provided as displacement time-history input functions. While ground motions were not recorded at all bents, they were measured at the abutments and at the base of Bent 5, in the vicinity of the expansion joint between frames. Thus the measured local ground displacements were rotated into global coordinates of the analysis model and interpolated between abutments and the base of Bent 5, in order to develop unique longitudinal and transverse input motions for the remaining bents.

A relatively simple spine model was developed for the entire connector bridge, consisting of beam elements for the superstructure, columns and large-diameter shafts. A more detailed shell model was also developed for Frame 1, which was identical to Frame 1 of the spine model, with the exception that the superstructure, bent caps and diaphragms were modeled with shell rather than beam elements. Initial comparisons between the shell and spine models revealed that something was wrong with one of the models, but it was not clear what was causing a difference of about 4% in the 1st mode response period (transverse bending of columns and torsion of superstructure) of the two models. Mass and stiffness values for the two models were within 1% of each other, and a 4% error in period indicates that one of these terms must be in error by the square of 1.04, or 8%.

After developing breakout spine and shell models of a single straight span with the cross-section of the connector bridge it was realized that the difference between the models was that the spine model had no rotational mass while the shell model naturally develops it due to the distribution of translational mass away from its centroidal axis. When this rotational mass was added to the breakout spine model, the torsional mode shape and period agreed with the breakout shell model. Based on these results, the rotational mass was calculated by hand and added to each of the superstructure nodes in the spine model. It was shown that by adding the rotational

mass of the superstructure, about its axis, to a spine model, time-history responses are improved and are very similar to the more detailed shell model and measured responses. With no rotational mass included, the overall time-history behavior drifted away from the more accurate shell model and measured bridge responses.

It was also found that in order to match the period of the structure and the measured time-history response, a 10% increase to the ACI modulus of elasticity [4] was required for a concrete strength of 5 ksi. The increase to the ACI modulus of elasticity recognizes that for the small stresses from the Hector Mine Earthquake, the concrete is near the beginning of its nonlinear stress-strain curve and that the initial tangent modulus of elasticity should be used rather than the softer secant ACI value. The initial tangent modulus is reported to be about 10% greater than the ACI value [5], which defines its secant value at 50% of the concrete strength. Analyses with concrete strengths of 4 ksi and 6 ksi were also performed, but comparisons to measured results indicate that the most realistic stiffness was based on the 5 ksi model. Comparisons between Frame 1 spine model results and measured results show that the most realistic overall damping level is 5%. Other damping levels investigated include 2% and 10%, followed by more refined damping levels of 3% and 4%.

Thus the results of this study have shown that (1) spine models can accurately capture time-history behavior of a connector bridge subjected to an earthquake, as demonstrated by direct comparisons to measured responses and the more detailed shell model, (2) damping levels of 5% used by Caltrans and others appears to be a reasonable value and (3) a concrete strength of 5 ksi is realistic for seismic design and analysis of concrete bridge structures, with a 10% increase to the modulus of elasticity for small load levels. The 10% increase to the ACI modulus of elasticity was used in the analyses presented here because the seismic loading was much smaller than the seismic levels expected in design. Therefore, for seismic bridge design, it is recommended that the modulus of elasticity still be based on the ACI expression without the 10% increase, as the concrete will be subjected to much larger stresses under the design level earthquake than the concrete of the North Connector was from the Hector Mine Earthquake.

An important discovery about the spine model was found by comparing spine model results to results from the more detailed shell model, which lead to the realization that the rotational mass of the superstructure and bent caps, about the axis of the superstructure, needed to be included in the model. This is because all of the mass of the superstructure runs along its spine, which has no thickness or height and, therefore, develops no rotational mass inertia. The shell model develops this rotational mass inertia quite naturally as the translational mass is distributed over the width and height of the section. It is recommended that in future analyses, Caltrans include the rotational mass of the bridge superstructure by lumping it at each node of the spine model. Bent cap rotational mass should also be added to the rotational mass of the superstructure, at the nodes where the columns and superstructure meet.

For single-column-bent structures, the rotational mass is significant to its dynamic response due to the rotation of the superstructure as it moves back and forth transversely. This will be amplified for long, multi-frame viaducts, with interior frames that do not have an abutment at either end to provide some restraint. This should not be a concern for multi-column-bent structures, as the superstructure will remain relatively flat as it moves transversely.

However, both multi-column-bent structures and long, multi-frame, single-column-bent viaducts should be investigated in the near future to provide insight into their seismic behavior and to give recommendations regarding these important structures.

In concluding, it is important to note that the bridge exhibited linear-elastic behavior when subjected to the relatively small ground shaking from the distant Hector Mine Earthquake. Thus the developed structural models were also linear-elastic, with excellent comparisons between time-history analysis results and the measured bridge response. From a larger earthquake, nonlinear behavior of the bridge is expected, including plastic hinging of the columns, banging of frames at the hinge and crushing of soil. It would be of great value to the engineering community if the present study, which showed that good linear-elastic dynamic results for a connector bridge can be achieved with relatively simple spine models and the more detailed shell models, was extended to model a bridge structure that was subjected to much larger ground motions so that nonlinear behavior of the bridge resulted.

The contents of this report were developed under Contract No. 1001-763 from the California Department of Conservation, California Geological Survey, Strong Motion Instrumentation Program. However, these contents do not necessarily represent the policy of that agency nor endorsement by the State Government.

References

1. McCallen, D. B., Romstad, K. M., *"Seismic Response Computations for a Simple Overcrossing", Proceedings, The Third Annual Seismic Research Workshop*, Sacramento, California, 1994.

2. SAP2000, Version 8, User's Manuals, Computers and Structures, Inc., Berkeley, California, 2002.

3. Caltrans Seismic Design Criteria, Version 1.2, Caltrans, Sacramento, California, 2001.

4. ACI *Building Code Requirements for Structural Concrete* (ACI 318-95), American Concrete Institute, Farmington Hills, Mich., 1995.

5. MacGregor, J. G., *Reinforced Concrete Mechanics and Design*, Prentice Hall, Upper Saddle River, N. J., 1997.

6. LPile Plus for Windows, Version 4.0, User's Manuals, ENSOFT, Inc., Austin, Texas, 2000

7. Dowell, R. K., *Time-History Analyses versus Measured Seismic Responses of the 5/14 Connector Bridge,* Report No. DH-04-02, Dowell-Holombo Engineering, Inc., San Diego, California, 2004.

Figure 1. North Connector, looking north

Figure 2. North Connector, looking northeast at Abutment 11

Figure 3. North Connector, looking east.

Figure 4. North Connector, looking east at hinge detail.

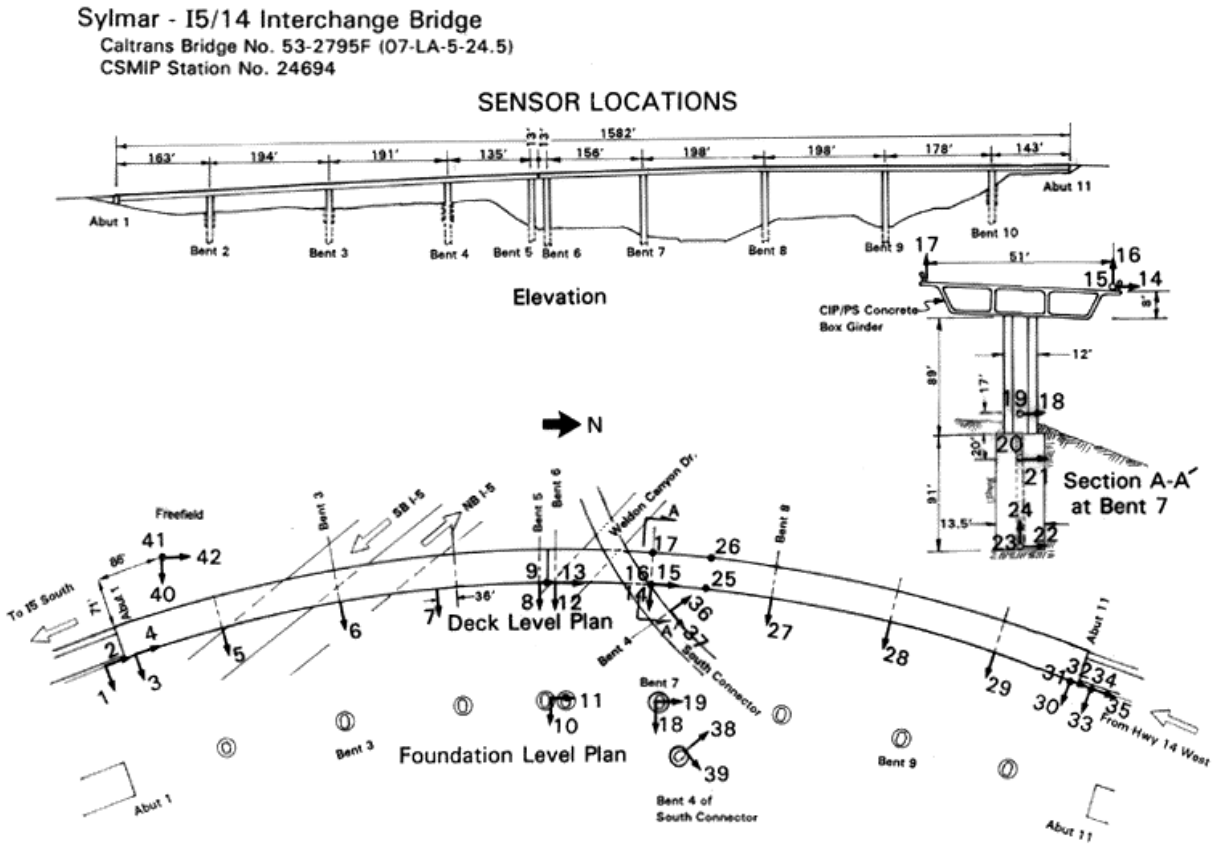

Figure 5. Bridge details and instrumentation layout

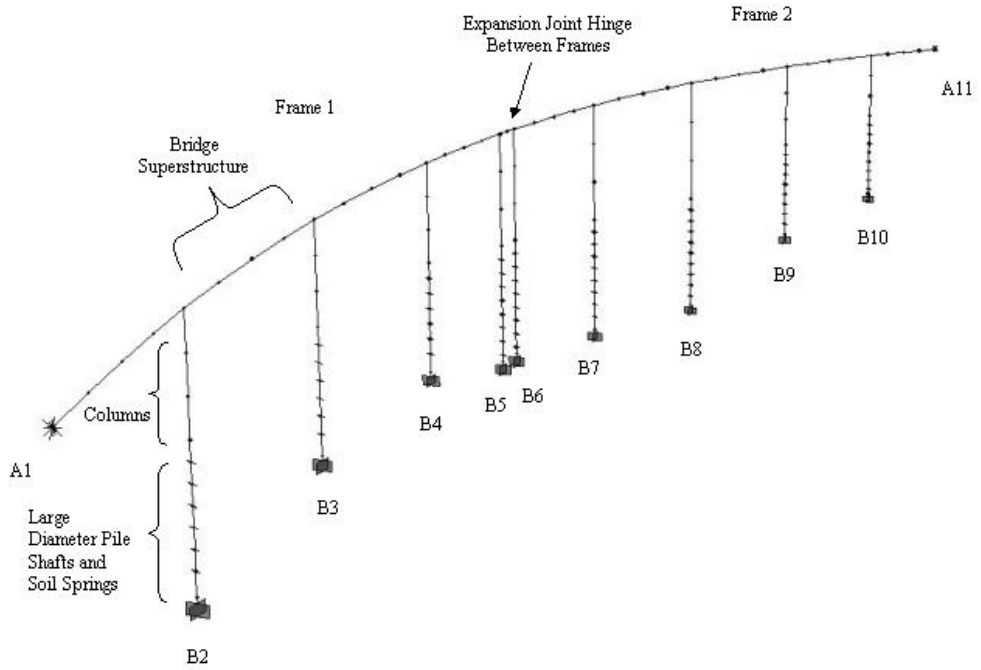

Figure 6. Isometric view of complete spine model of North Connector Bridge

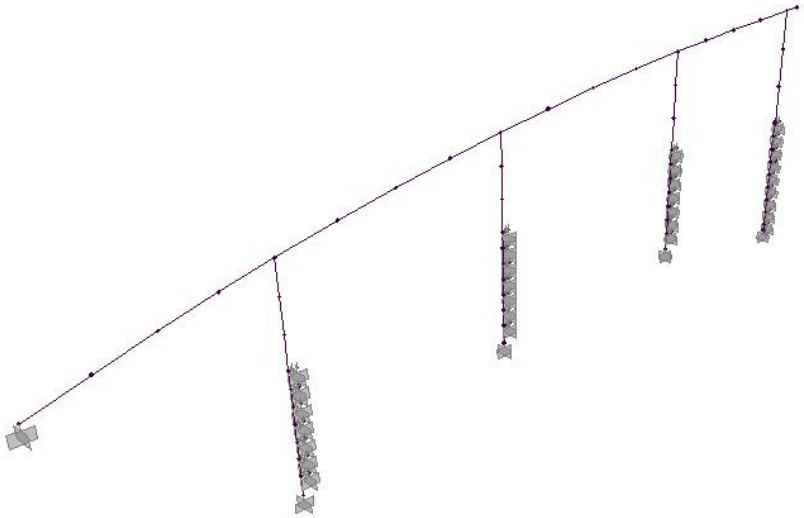

Figure 7. View of Frame 1 spine model from above looking northwest

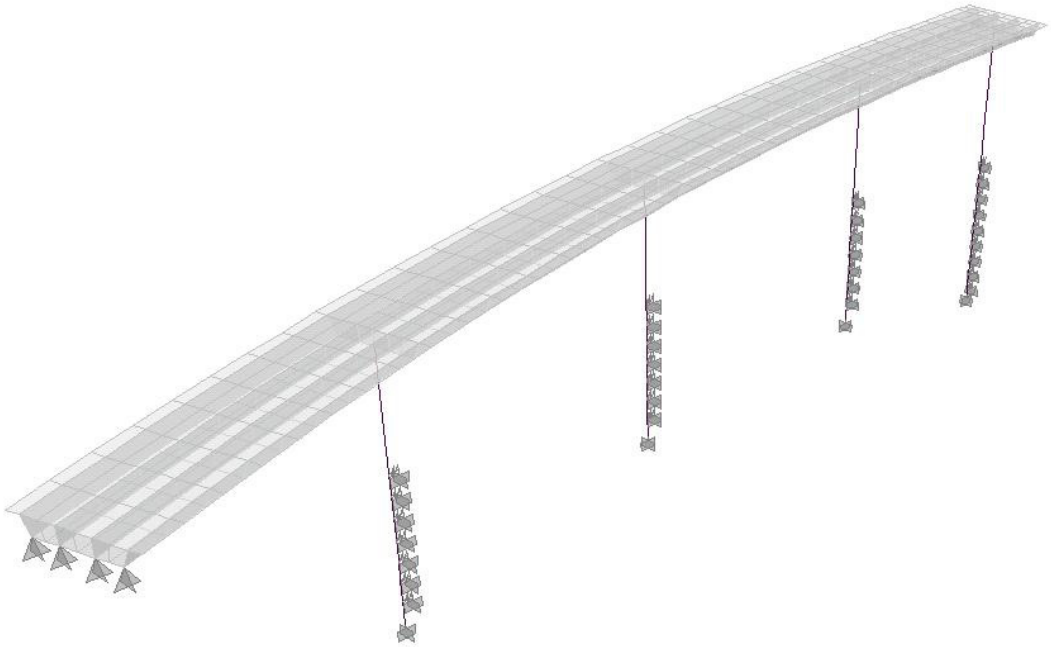

Figure 8. View of Frame 1 shell model from above looking northwest

T_n = 1.056 seconds T_n = 1.052 seconds

(a) Mode 1 (transverse/torsion)

T_n = 0.688 seconds T_n = 0.661 seconds

(b) Mode 2 (double transverse)

T_n = 0.485 seconds T_n = 0.493 seconds

(c) Mode 3 (vertical)

Figure 9. Modes 1 through 3, Frame 1 shell and spine models

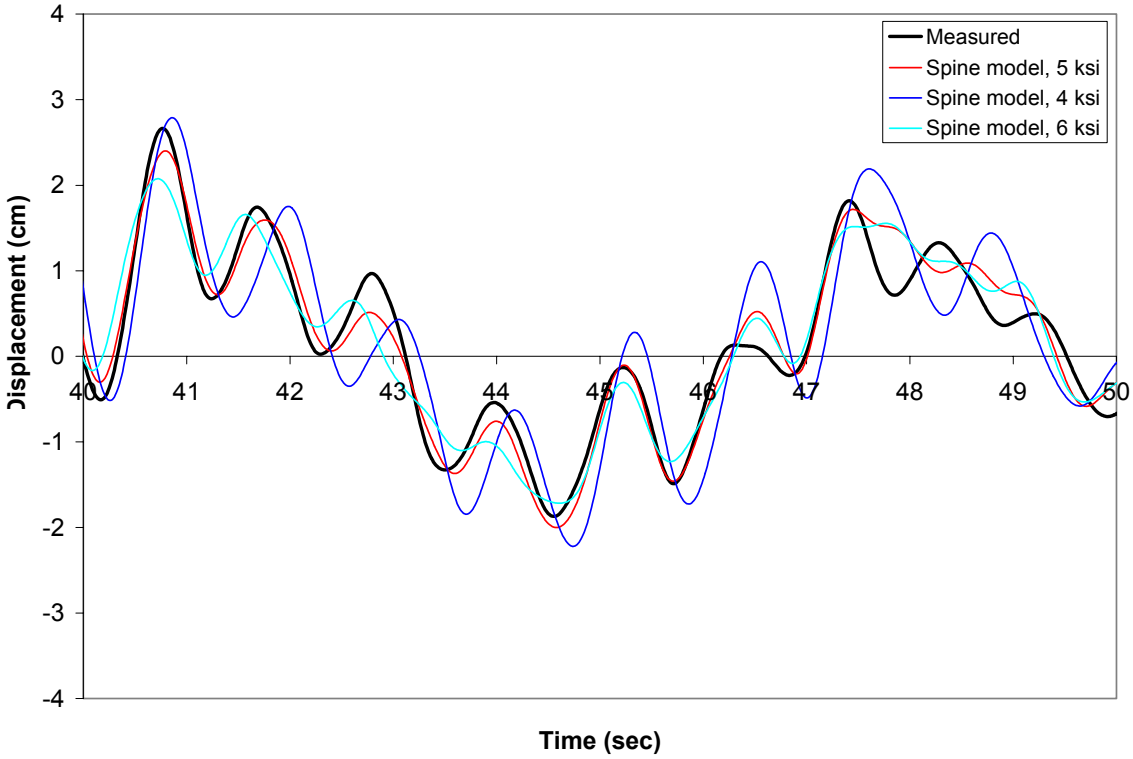

Figure 10. Transverse Bent 5 responses, 4, 5 and 6 ksi concrete (40-50 sec)

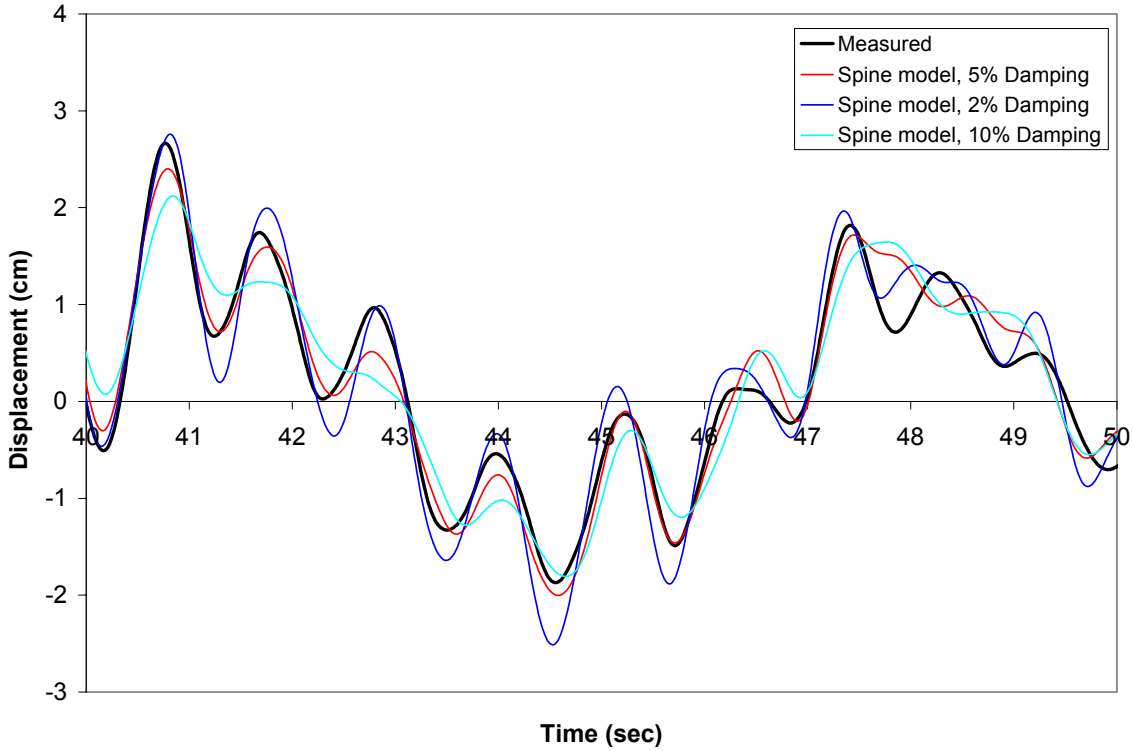

Figure 11. Transverse Bent 5 responses, 2%, 5% and 10% damping (40-50 sec)

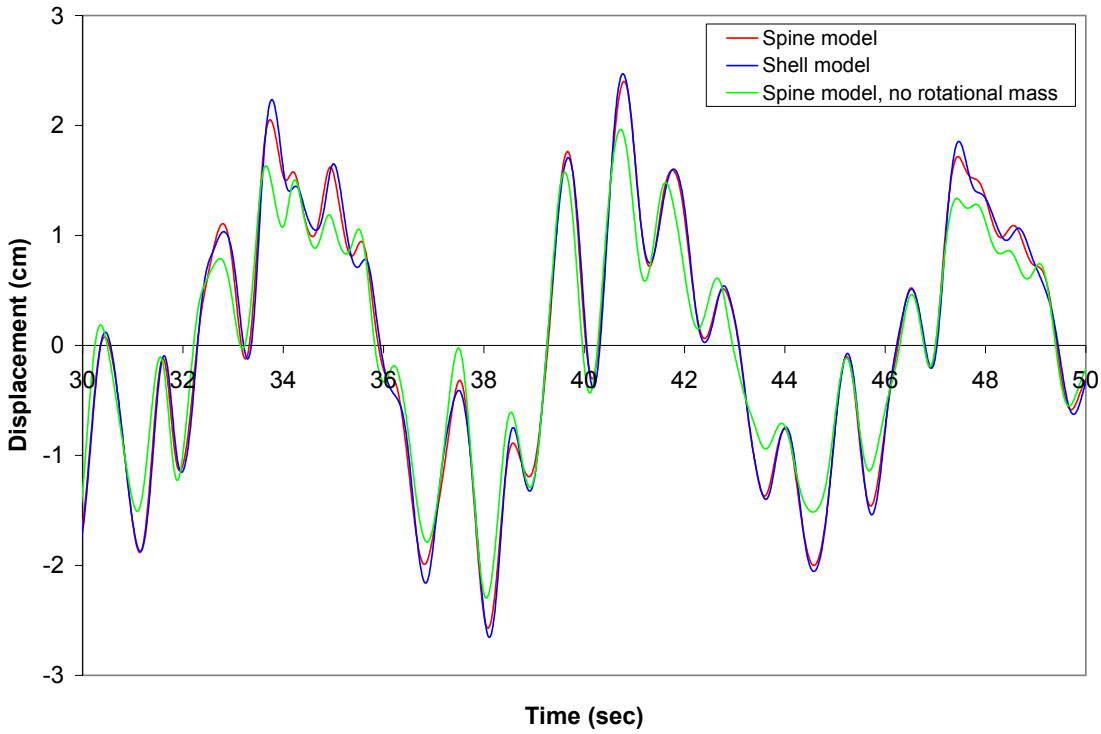

(a) Absolute displacements

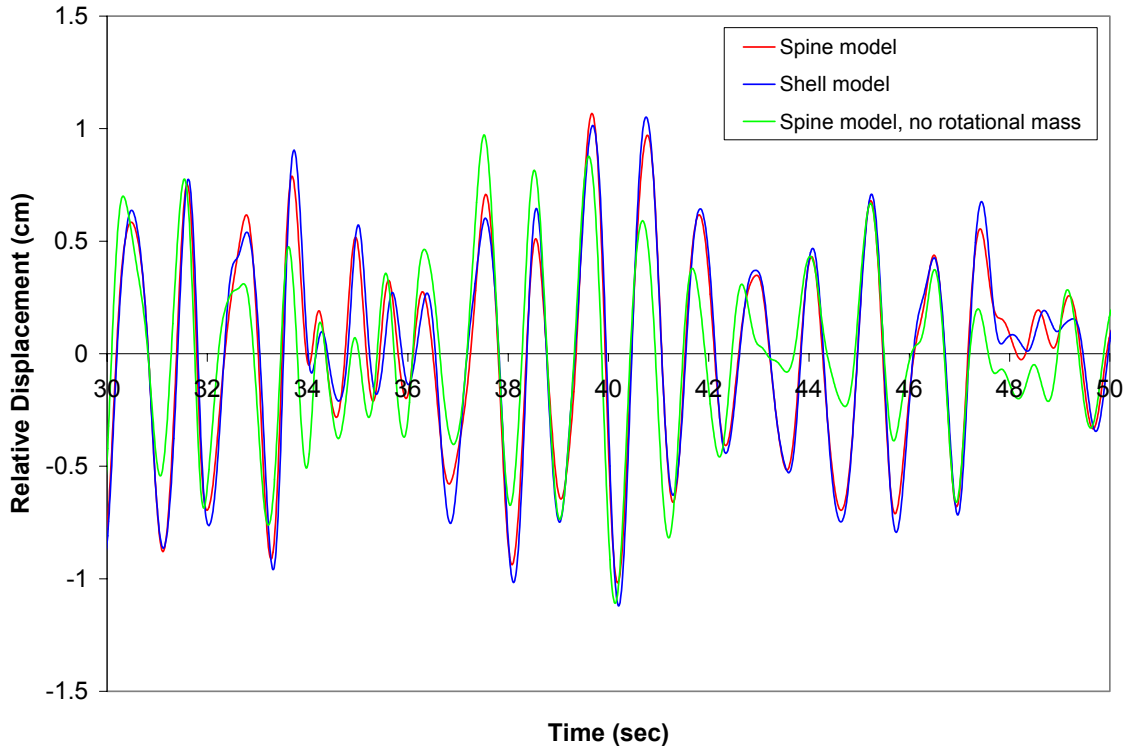

(b) Relative displacements

Figure 12. Transverse Bent 5 responses, shell model vs. spine model with and without rotational mass of superstructure included (30-50 sec)

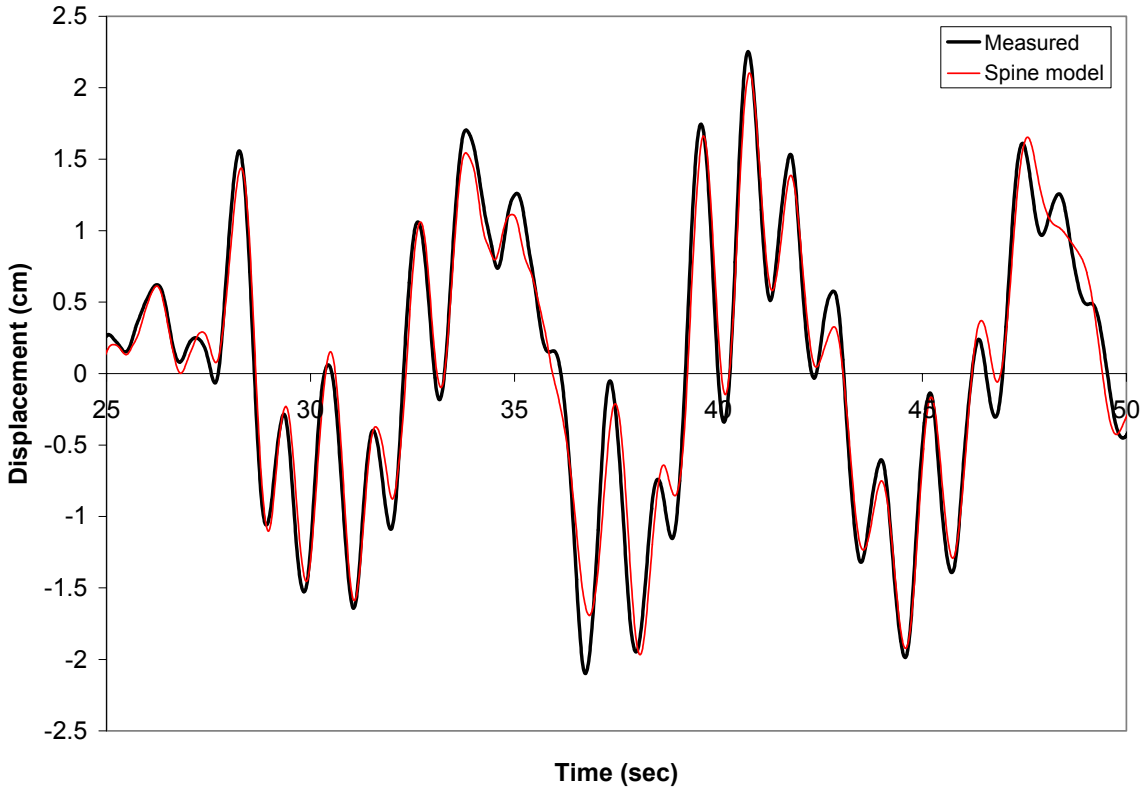

(a) Absolute displacements

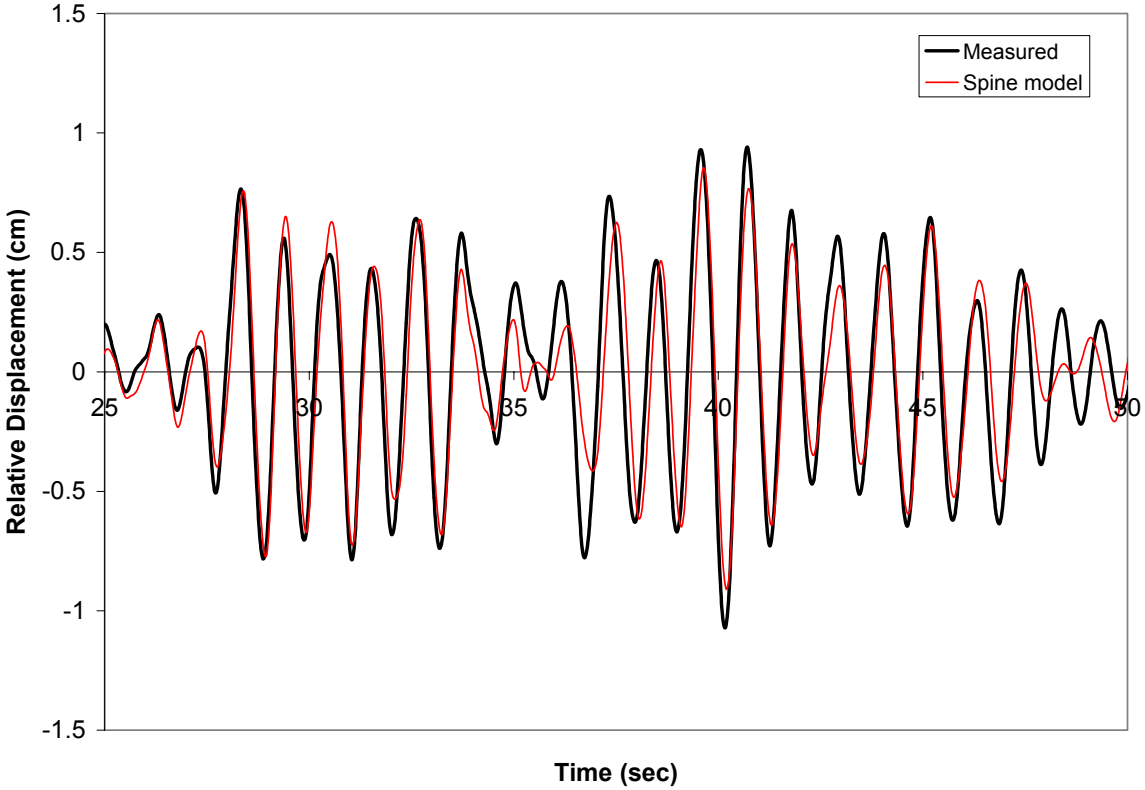

(b) Relative displacements

Figure 13. Spine model and measured transverse displacements at Bent 4 (25-50 sec)

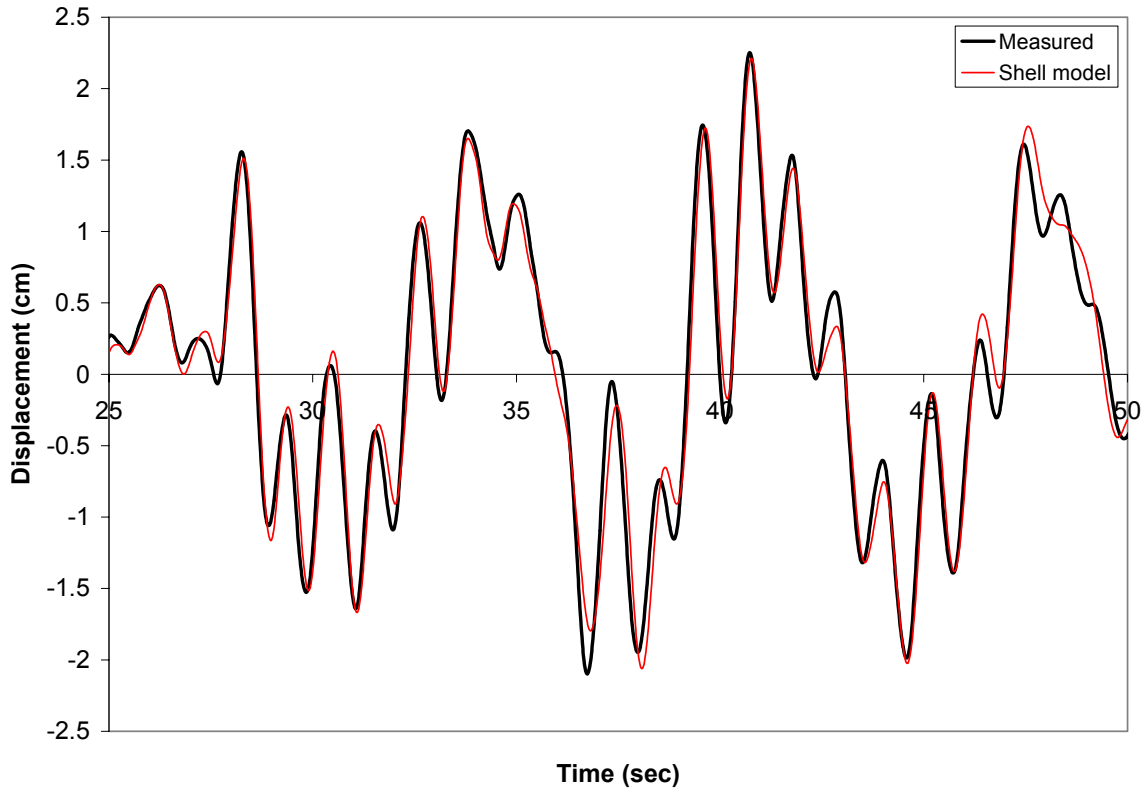

(a) Absolute displacements

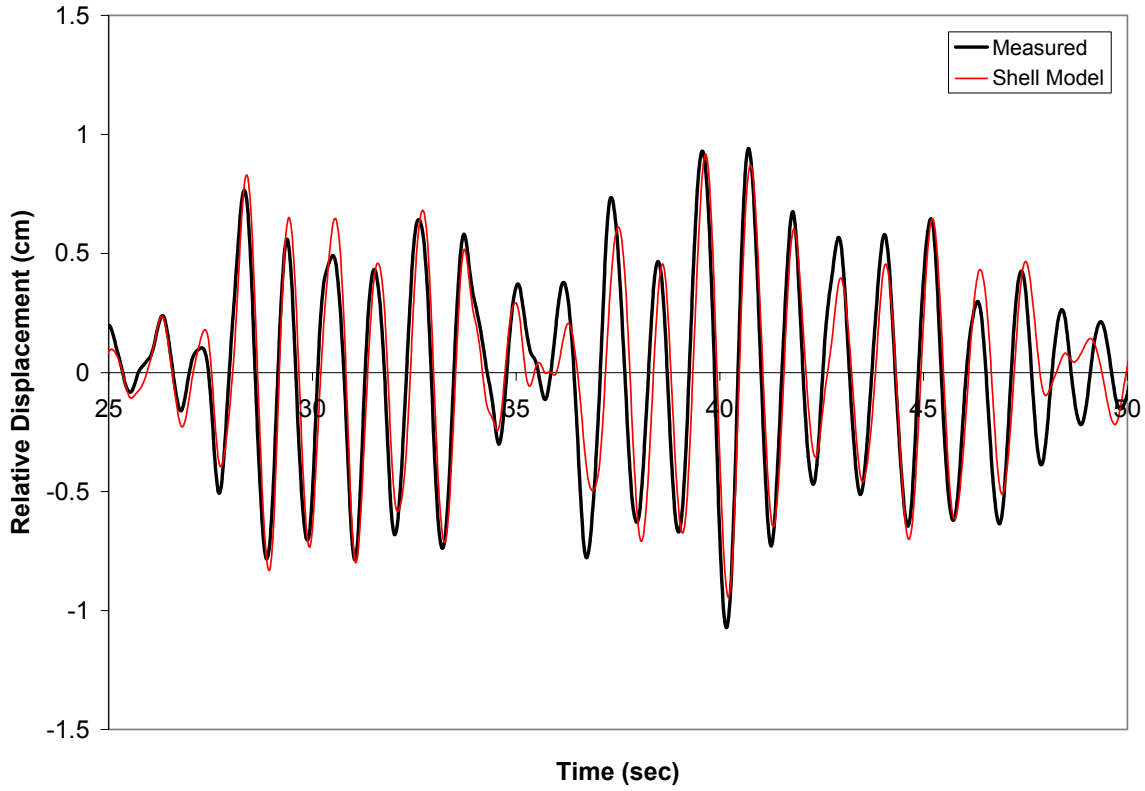

(b) Relative displacements

Figure 14. Shell model and measured transverse displacements at Bent 4 (25-50 sec)

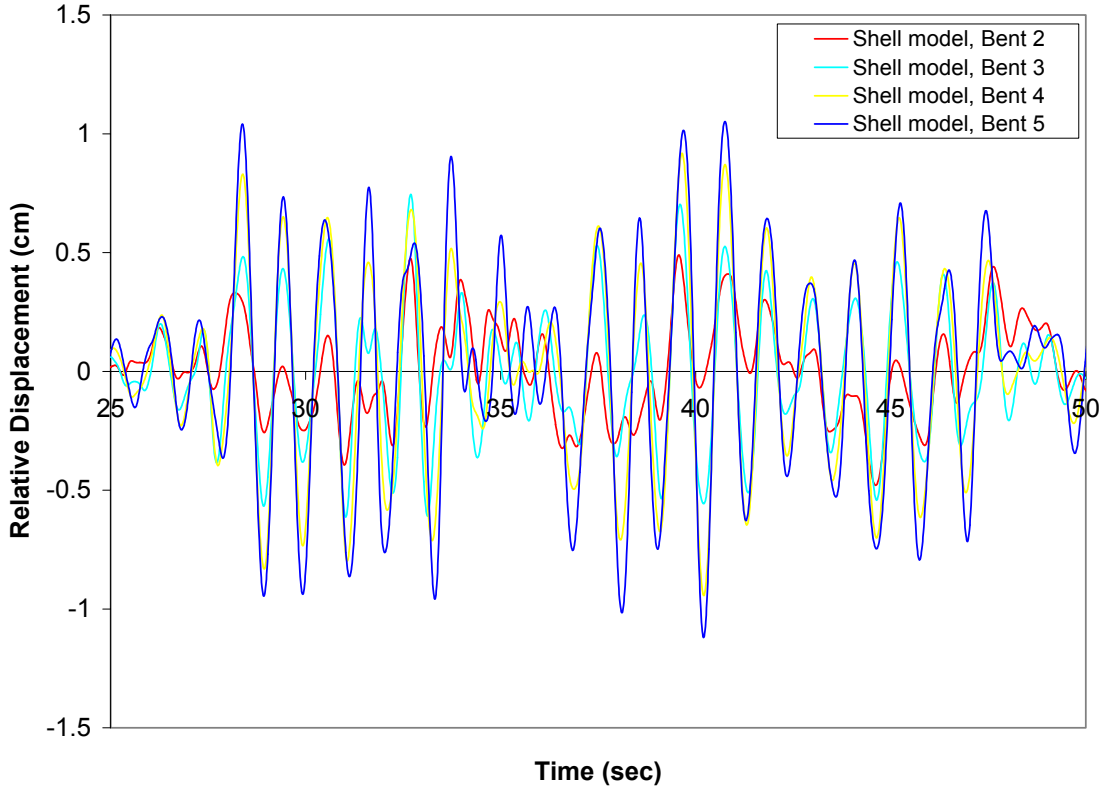

(a) Shell model

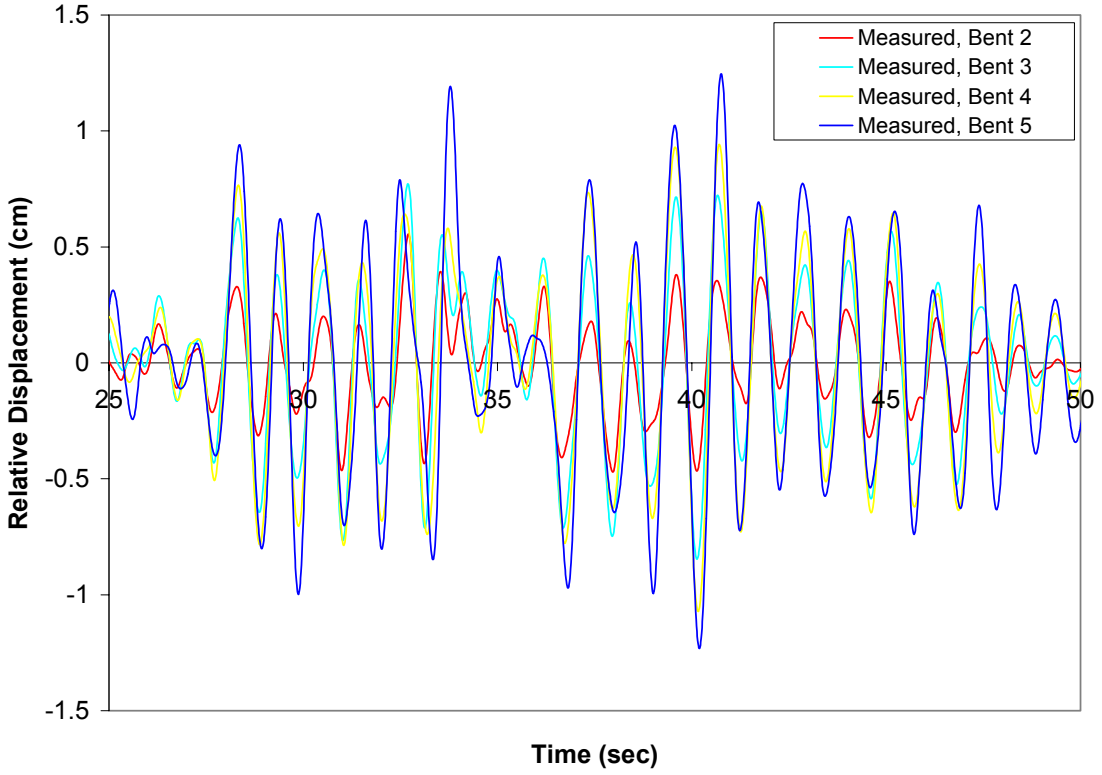

(b) Measured

Figure 15. Shell model and measured relative transverse motions of Frame 1 (25-50 sec)